

IN SILICO DESIGN OF NOVEL PEPTIDES FOR TREATING CANCER THROUGH INHIBITION OF THE RANK-TRAF6 INTERACTION

Sara Batalha Galhofo Celestino Perdigão

Master Student in Pharmaceutical Engineering at Instituto Superior Técnico, Universidade de Lisboa, Av. Rovisco Pais, 1, 1049-001, Lisboa, Portugal

Abstract

The RANK-TRAF6 metabolic pathway is commonly associated with osteoporosis and development of breast and prostate cancer. Therefore, the inhibition of binding between RANK and TRAF6 has been studied. One of the hypotheses is through decoy peptides that bind to one of the targets blocking the binding. The aim of this thesis is the prediction of decoy peptides based on RANK that binds to TRAF6 and their synthesis. The 3D structures of the selected peptide-based sequences were predicted, and a molecular docking study was performed to analyze and validate their stability with TRAF6. Molecular docking assessment was done through a balance between HADDOCK score, percentage of residues at the interface and the RMSD, allowing to reach the most stable complex for each peptide. The peptides were synthesized in solid phase, followed by purification by RP-HPLC, and a purity >95% was obtained for all peptides. Biological studies will be further performed to evaluate their efficiency in inhibiting RANK-TRAF6 binding.

Keywords: TRAF6, Protein-Protein Interaction, Computational Chemistry, HADDOCK score, Solid-Phase Peptide Synthesis, Reverse-Phase High Performance Liquid Chromatography

Introduction

According with the World Health Organization (WHO) in 2020, 10 million deaths were counted due cancer, where 2.26 million were from breast cancer and 1.41 million from prostate cancer[1]. Studies show relationship between breast and prostate cancer with the propensity to metastasize to bone[2]. The structural and metabolic integrity of bone is maintained through the dynamic process of bone remodeling, by two main kinds of bone cells, osteoblasts and osteoclast, osteoblasts are responsible for the formation of new bone and osteoclasts for bone resorption[3]. When cancer cells block this process, they speed up the action, meaning there is an increase in the activity of regulators of bone causing osteolysis and abnormal new bone formation[4][5]. Currently, no efficient therapy or treatment has been found yet, so there are

several therapeutic targets for it, namely the receptor activator of nuclear factor-kappa β (RANK) signaling pathway[6][7]. This pathway is important because it is responsible for osteoclast activation, and as previously mentioned, breast and prostate cancer have a propensity to metastasize to bone.

NF- $\kappa\beta$ is a heterodimer composed of two subunits, p65 and p50, and he is inactivated in the cytoplasm bound to the inhibitor Kappa-beta (i $\kappa\beta$) protein, forming the NF- $\kappa\beta$ /i $\kappa\beta$ complex[8][9]. To activate NF- $\kappa\beta$ an extracellular stimulus is needed. Afterward an intracellular pathway is activated leading to the activation of NF- $\kappa\beta$. After its activation, NF- $\kappa\beta$ will cross to nucleus, binding to a specific DNA and activate the expression of the target gene responsible for osteoclast formation, and carry out its transcription[8][10].

Extracellular stimulation resides in the protein-protein interaction between RANK and its ligand

RANKL, members of tumor necrosis factor (TNF) cytokine family. However, the same interaction needs to be mediated by TNF receptor-associated factors (TRAFs) for an intracellular signaling pathway be activated. This way NF-KB is recruited, subsequently by intermediate factors NF-K β is free in the cytoplasm and then enters in the nucleus and carry out the target gene, leading to the activation of osteoclasts[10][11].

TRAFs were first discovered as adaptor proteins that couple the tumor necrosis factor receptor family to signaling pathways[12]. Among all seven TRAFs, TRAF6 is the only one that can activate NF-K β , because although TRAF6 has the same structural characteristics of the other members of the family, he is the less conserved in is TD, more specifically in the TRAF-C domain, since he only shares 30 % of the sequence identity with the others TRAFs members (1-5). So he does not have the same binding site as the others, meaning that TRAF6 binds in a different region of the RANK than TRAFs 1, 2, 3, 5 and 7 [12][13][14].

In order to reach the TRAF6 binding motif, several studies and hypotheses were conducted, a sequence alignment based on the structure of TRAF6 binding sites in mouse and human, was performed. Based on that sequence alignment it was able to conclude that TRAF6 binding motif, in RANK (TRANCE-R), and other TNFR family members, is a generalized amino acid sequence pattern, designated Pro-X-Glu-X-X-(Ar/Ac). Were Ar is an aromatic and Ac an acid residue. The residue Glu have been designated in position P₀, Pro in position P₂ and Ar/Ac in position P₃. These residues are the most crucial for TRAF6 interaction and essential for maintaining the integrity of the interface[15][13].

Which lead us to the aim of this thesis, the synthesis of peptides that inhibit RANK-TRAF6 binding. For that *in silico* methods were used to predict 3D structure of the selected peptides and then submitted to a molecular docking in order to understand how occurs the interaction with TRAF6 and validate their stability.

Materials and methods

Decoy peptides

Ann T. Poblenz suggests that T6DP3 (RKIPTEDEY) is the most effective RANK-TRAF6 peptide inhibitor[16].

Based on this study, 4 sequence-based peptides were designed. The difference between Peptide 1 and Peptide 2 is the alanine mutation at active residues that are experimentally described as important in the interaction RANK-TRAF6. Thus, it is possible to check if they are really key residue. Peptide 3 and Peptide 4 have the same sequence of Peptide 1 and 2 plus a Cell Penetrating Peptides (CPP) which will facilitate the internalization of peptide into cell. The CPP used is, AAVALLPAVLLALLAP, a hydrophobic sequence of the Kaposi fibroblast growth factor signal peptide. The sequence of four peptides are present in table 1.

TABLE 1: PEPTIDES TO BE PRODUCED.

Peptide	Sequence
Peptide 1	RKIPTEDEY
Peptide 2	RKIATADEA
Peptide 3	AAVALLPAVLLALLAP RKIPTEDEY
Peptide 4	AAVALLPAVLLALLAP RKIATADEA

Computational Chemistry

3D structure prediction

PEP-FOLD 3 and I-TASSER webserver will be used to predict 3D structures of Peptide 3 and 4. As I-TASSER only predicts structures longer than 10 amino acids, PEPstrMOD webserver will be used to predict the tertiary structure of Peptide 1 and 2. The five best models for each sequence will be analysed in the ProSA-Web webserver, which allows us to select the best and most robust model[17][18][19][20][21][22][23][24][25][26].

Molecular Docking

The molecular docking study was performed using the HADDOCK (High Ambiguity Driven protein-protein DOCKing) server[27][28].

HADDOCK starts with a randomization of orientations and rigid body energy minimization (1000 solutions), then occurs semi-rigid simulated annealing in torsion angle space (200 solutions), finally occurs a refinement in Cartesian space with an explicit solvent (200 solutions). HADDOCK also uses biological information to drive docking, introducing ARIs (Ambiguous Interaction Restraints).

Two docking runs were performed for each peptide, where in the first docking the active residues chosen for Peptides 1, 2, 3 and 4 are those that are experimentally described as important in the interaction with the TRAF6 and in the second docking all residues belonging to the peptides are considered active (table 2).

Beyond the HADDOCK score, the top 10 was analyzed according to their percentage of interfacial residues and RMSD. The HADDOCK score is provided by HADDOCK allowing to perceive which is the most stable complex obtained through an energies algorithm; the percentage of interface residues is calculated considering: i) the active residues that are experimentally described as important in the interaction with the TRAF6 protein (TRAF6_Seq_1; TRAF6_Seq_2; TRAF6_Seq_3 and TRAF6_Seq_4) and ii) all residues of the peptide sequence. (TRAF6_Seq_1_1, TRAF6_Seq_2_1, TRAF6_Seq_3_1 and TRAF6_Seq_4_1). The RMSD was calculated in PyMOL, where the complex with the lowest RMSD is the most similar to crystal (1LB5).

Solid-Phase Peptide Synthesis

Solid-phase peptide synthesis

Two Resins were used, Rink Amide MBHA resin (Novabiochem®) with a substitution coefficient of

0.78 mmole/g, used for peptide 1, and Rink Amide MBHA resin (Novabiochem®) with a substitution coefficient of 0.38 mmole/g used for peptide 2, 3 and 4.

The resin was weighed and transferred to the polymeric reactor. The resin was swollen, where it was washed three times with DMF (CARLO ERBA reagents) and three times with DCM (CARLO ERBA reagents), respectively. After swelling, the resin was deprotected with 4 mL of 20 % piperidine (SIGMA-ALDRICH®) solution in DMF, this was added to the reactor and it was sealed and taken to an ultrasonic bath for 5 to 10 min. After this, the deprotection solution was discarded and the resin was washed with DMF and DCM (three times). At the end of deprotection, a Kaiser test was performed.

The first amino acid was conjugated with a solution containing 3.5 amino acid equivalents and 3.5 equivalents of HBTU (activator) (Iris Biotech GmbH) in 1mL of DMF solution, the solution was taken to an ultrasonic bath for 5 min to promote amino acid activation. 10 equivalents of DIPEA (activating base)(SIGMA-ALDRICH®) were added to the solution and taken to the ultrasonic bath for 1 min. The solution was transferred to the reactor where the first amino acid goes coupling for 10 min in the ultrasonic bath. After conjugation, the solution is removed and the resin is washed. At the end of each coupling, a kaiser test was performed and then the deprotection of the amino acid is carried out in order to conjugate the next one. This is repeated until the end of the peptide chain is reached. All amino acid used were from Novabiochem®.

TABLE 2: CONDITIONS FOR EACH DOCKING.

	<i>Run Name (ID)</i>	<i>Resíduos Activos Chain A → TRAF6</i>	<i>Resíduos Activos Chain B → Peptídeos</i>	
Resíduos ativos dos peptídeos são os descritos pela literatura	TRAF6-Seq_1	392, 410, 473, 471, 432, 459	4,6,9	
	TRAF6-Seq_2		4,6,9	
	TRAF6-Seq_3		20,22,25	
	TRAF6-Seq_4		20,22,25	
Todos os resíduos do peptídeo são considerados ativos	TRAF6-Seq_1_1			1,2,3,4,5,6,7,8,9
	TRAF6-Seq_2_1			1,2,3,4,5,6,7,8,9
	TRAF6-Seq_3_1			1,2,3,4,5,6,7,8,9, 10,11,12,13,14,15, 16,17,18,19,20,21, 22,23,24,25
				1,2,3,4,5,6,7,8,9, 10,11,12,13,14,15, 16,17,18,19,20,21, 22,23,24,25
	TRAF6-Seq_4_1			1,2,3,4,5,6,7,8,9, 10,11,12,13,14,15, 16,17,18,19,20,21, 22,23,24,25

The final step is the cleavage of the peptide, where the resin with the chain was swollen, deprotected, followed by a Kaiser test. After these steps, a 4 mL cleavage solution (cocktail) was prepared containing 95 % trifluoroacetic acid (TFA)(3.8 mL) (SIGMA-ALDRICH®) 2.5 % deionized water (0.1 mL) and 2.5 % triisopropylene (TIS)(0.1 mL)(SIGMA-ALDRICH®). Then the solution was added to the reactor and left for four hours in constant agitation, after the liquid was transferred to a falcon, where the excess of TFA was evaporate by nitrogen flow. Ether was added to the falcon in a 1:10 ratio of TFA to ether, it was homogenized and then it was centrifuged (centrifuge HERMLE) for 5 minutes at 5000 rpm and an acceleration of 5. The precipitated peptide was separated from the supernatant. The process of ether addition, centrifugation and removal of the supernatant was repeated three times. At the end of the third time, the excess ether was removed and finally the nitrogen dried peptide was obtained.

Kaiser test was used to monitor the synthesis. In a teste tube containing a few dry resin spheres

were added two drops of three different solutions: A (5 g of ninhydrin in 100 mL of ethanol); B (80 g of phenol in 20 mL of ethanol) and C (2 mL of 0.001 M of aqueous potassium cyanide (KCN) in 98 mL of pyridine). The tube was placed in a water bath for 5 to 10 minutes, after the resin spheres were thoroughly observed.

Peptides biological characterization and purification

Reverse-Phase Analytical High Performance Liquid Chromatography (RP-HPLC)

A solution with 200 µL of water with 0.1% TFA was prepared with a small portion peptide. Sometimes it is necessary to add one or two drops of ACN (CARLO ERBA REAGENTS®). We took about 35 µL of the solution of each peptide and injected it into the analytical RP-HPLC, the time between runs is about 45-50 min, depending on the method used. The system is composed with a pump (PerkinElmer® 200 Series Pump), a detector (PerkinElmer® 200 Series UV/Vis), a degasser (PerkinElmer® 200 Series vacuum degasser) and a column (Supelco Analytical,

Discovery® BIO Wide Pore C18-5, 25 cm X 4.6 mm, 5 µm, SIGMAALDRICH®). The UV detection was between 210 nm to 220 nm, the eluents used in the system were H₂O with 0.1% TFA and ACN in 0.1% TFA, in channel A and B, respectively. Having peptides with different sizes, two HPLC methods were optimized, one for the smaller ones and the other for the larger ones, both methods are described in table 3 and 4.

TABLE 3: OPTIMISED METHOD FOR THE SMALLEST PEPTIDES (PEPTIDE 1 AND 2).

Time (minutes)	Eluent A (%)	Eluent B (%)	Flow (ml/min)
-	95	5	1
3	95	5	
28	75	25	
30	0	100	
33	0	100	
35	95	5	

TABLE 4: OPTIMISED METHOD FOR THE MAJOR PEPTIDES (PEPTIDE 3 AND 4).

Time (minutes)	Eluent A (%)	Eluent B (%)	Flow (mL/min)
-	90	10	1
3	70	30	
28	40	60	
30	0	100	
33	0	100	
35	90	10	

Reverse-Phase Preparative High Performance Liquid Chromatography (RP-HPLC)

A solution with 10 mL of H₂O with 0.1% TFA was prepared with a small portion peptide, the volume injected was 1000 µL. The system is composed with a pump (Waters 2535 Quaternary Gradient Module), a detector (Waters 2998 Photodiode Array Detector), a degasser (Uniflows, DG- 3210) and a column semi-preparative (MACHEREY-NAGEL Nucleosil® 100-5 C18, 250 cm x 8 cm). The UV detection was between 210 nm and 220 nm, the eluents used in the system were H₂O with

0.1% TFA and ACN in 0.1% TFA, in channel A and B, respectively. The HPLC methods used were the same as applied in the analytical part. During purification, three fractions of the pure peptide are removed and then lyophilized (CoolSafe 100-9 Pro).

Mass Spectrometry (MS)

Analysis by electrospray mass spectrometry (ESI-MS) of compounds was performed with the aid of an electrospray ionization (ESI) mass spectrometer (Bruker HCT Esquire 3000 plus®). This analysis was performed according to the methodology developed by the research group of Radiopharmaceutical Sciences from Center for Nuclear Sciences and Technologies (C²TN).

The molecular weight of each peptide was calculated through ExPASy and the molecular ions of each peptide were then calculated by hand [29][30][31].


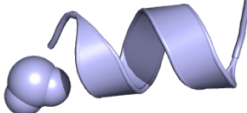
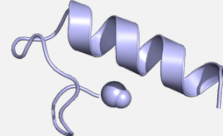
Results and discussion

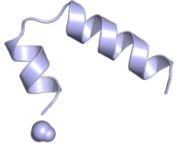
Computational Chemistry

3D structure prediction

Five models were generated for each peptide. They were further analyzed in the ProSA-Web webserver according to their z-score and visualized in the PyMOL to observe their structure. The models selected as well as their z-score are shown in table 5 [26][25].

TABLE 5: FINAL 3D STRUCTURE OF EACH PEPTIDE AND Z-SCORE.

Peptide	z-score	Final Structure
Peptide 1	- 1.42	
Peptide 2	- 1.40	
Peptide 3	- 4.86	

Peptide 4	- 3.22	
--------------	--------	---

These final structures will be used in molecular docking studies.

Molecular Docking

The 10 best complexes were selected according to the HADDOCK score considering that the more negative the better [27][28]. A balance between the three parameters described above allowed to select the most stable complex from each peptide. The chosen complexes are described in table 7.

Synthesis, Characterization and Purification of Peptides

After synthesis, characterization, evaluation and purification of the peptides were performed. The chromatograms of the synthesized peptides after purification are illustrated in figure 1.

In figure 1, the retention time of peptide 1 is longer than the retention time of peptide 2, 17.40 minutes and 11.35 minutes, respectively. This difference may be related to the fact that the peptide sequences are different.

The retention times of peptide 3 and 4 are very close, 18.86 minutes and 18.71 minutes, respectively. The proximity of the retention times is not only due to the similarity between the two peptide chains, where the mutated active residues are the same as in peptides 1 and 2, but also possibly due to their peptide sequence being

longer (25 amino acids) and these mutated amino acids does not interfere.

Table 5 shows the purities of each peptide.

TABLE 5: PURITY OF EACH AMINO ACID AFTER PURIFICATION.

Peptide	Sequence	Purity (%)
Peptide 1	RKIPTED EY-NH ₂	96
Peptide 2	RKIATADEA-NH ₂	99
Peptide 3	AAVALLPAVLLALLAP RKIPTED EY- NH ₂	97
Peptide 4	AAVALLPAVLLALLAP RKIATADEA- NH ₂	>99

Based on table 5, it can be concluded that all 4 peptides are pure (>95%).

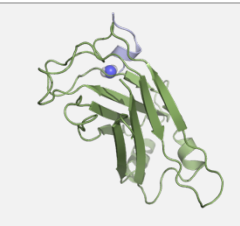
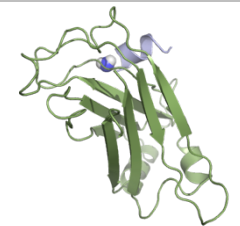
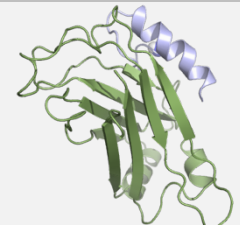
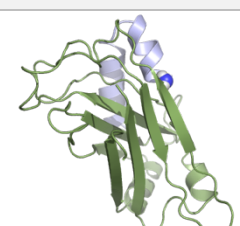
ESI-MS was performed to validate the presence of the peptide. The m/z ratio of each peptide is shown in table 6.

TABLE 6: M/Z RATIO OF EACH PEPTIDE OBTAINED BY ESI-MS.

Peptide	m/z		
	[M+1H ⁺] +	[M+2H ⁺] ²⁺	[M+3H ⁺] ³⁺
Peptide 1	1149,6	575,4	-
Peptide 2	973,6	487,3	-
Peptide 3	-	1324,5	883,5
Peptide 4	-	1236,4	824,6

Through table 6, it is possible to conclude that all peptides were present in the sample, since their molecular ions were found.

TABLE 6: FINAL COMPLEX OF EACH PEPTIDE.

Peptide	Complex	Final Structure
TRAF6_Seq_1_1	Complex_154w	
TRAF6_Seq_2_1	Coplex_9w	
TRAF6_Seq_3_1	Complex_109	
TRAF6_Seq_4_1	Complex_50w	

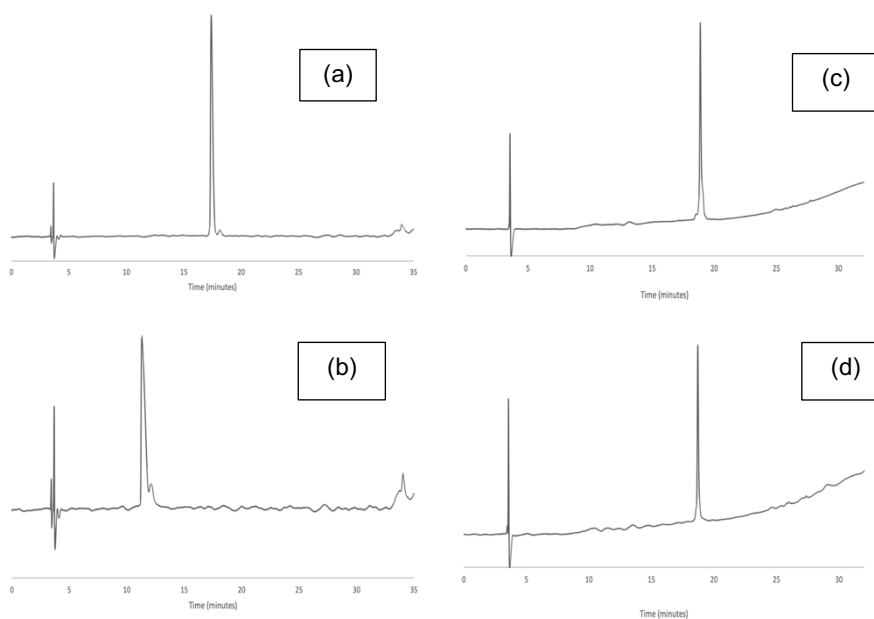


FIGURE 1: HPLC CHROMATOGRAM: (A) PEPTIDE 1, (B) PEPTIDE 2, (C) PEPTIDE 3 AND (D) PEPTIDE 4.

Conclusion

The aim of this work was the Prediction of the 3D structure, selection and synthesis of peptides that potentially inhibit the RANK-TRAF6 interaction.

3D structures of each peptide were predicted, and were subjected to molecular docking in order to predict the best pose of the complexes (peptides-TRAF6). Through the simulations performed, a balance between the parameters HADDOCK score, interfacial residues percentage and RMSD, allowed the choice of the most stable complex.

The synthesis of all peptides was successfully with >95% of purity, making them ready to be further used in *in vitro* studies.

This work served as a kickoff for the molecular dynamics' simulation studies of the studied complexes. Thus, through these computational tools, we can understand at the atomic level how the peptides interact with the target protein. Next, the evaluation of the biological ability of the synthesized peptides to interact with the TRAF6 will be made. Finally, and if the results are promising, *in vivo* studies will allow a better understanding of the behavior of these peptides in the biological systems.

References

1. World Health Organization Available online: <https://www.who.int/news-room/fact-sheets/detail/cancer> (accessed on Aug 5, 2021).
2. National Cancer Institute Available online: <https://www.cancer.gov/about-cancer/understanding/what-is-cancer#definition> (accessed on Aug 5, 2021).
3. American Cancer Society Available online: <https://www.cancer.org/treatment/understanding-your-diagnosis/advanced-cancer/bone-metastases.html> (accessed on Aug 5, 2021).
4. Guise, T.A.; Mohammad, K.S.; Clines, G.; Stebbins, E.G.; Wong, D.H.; Higgins, L.S.; Vessella, R.; Corey, E.; Padalecki, S.; Suva, L.; et al. Basic Mechanisms Responsible for Osteolytic and Osteoblastic Bone Metastases. *Am. Assoc. Cancer Res.* **2006**, *12*, 6213–6217, doi:10.1158/1078-0432.CCR-06-1007.
5. American Cancer Society Available online: <https://www.cancer.org/cancer/cancer-basics/what-is-cancer.html> (accessed on Aug 5, 2021).
6. Zhang, X. Interactions between cancer cells and bone microenvironment promote bone metastasis in prostate cancer. *Cancer Commun.* **2019**, *39*, 1–10, doi:10.1186/s40880-019-0425-1.
7. González-Suárez, E.; Sanz-Moreno, A. RANK as a therapeutic target in cancer. *FEBS (Federation Eur. Biochem. Soc.) Journal* **2016**, *283*, 2018–2033, doi:10.1111/febs.13645.
8. Glezer, I.; Marcourakis, T.; Avellar, M.; Gorenstein, C.; Scavone, C. O fator de transcrição NF- κ B nos mecanismos moleculares de ação de psicofármacos. *Rev. Bras. Psiquiatria* **2000**, *22*, 26–30.
9. Gohda, J.; Akiyama, T.; Koga, T.; Takayanagi, H.; Tanaka, S.; Inoue, J. RANK-mediated amplification of TRAF6 signaling leads to NFATc1 induction during osteoclastogenesis.

- EMBO (European Mol. Biol. Organ. J.* **2005**, *24*, 790–799, doi:10.1038/sj.emboj.7600564.
10. Pereira, M. *List of Equations 1, Universidade Nova de Lisboa, 2018.
 11. Xu, H.; Chen, F.; Liu, T.; Xu, J.; Li, J.; Jiang, L. Ellagic acid blocks RANKL – RANK interaction and suppresses RANKL-induced osteoclastogenesis by inhibiting RANK signaling pathways. *Chem. Biol. Interact.* **2020**, *331*, 109235, doi:10.1016/j.cbi.2020.109235.
 12. Bradley, J.R.; Pober, J.S. Tumor necrosis factor receptor-associated factors (TRAFs). *Nat. Publ. Gr.* **2001**, *1*, 6482–6491.
 13. Park, H.H. Structure of TRAF Family: Current Understanding of Receptor Recognition. *Front. Immunol.* **2018**, *9*, 1–7, doi:10.3389/fimmu.2018.01999.
 14. Xu, L.; Li, L.; Shu, H. TRAF7 Potentiates MEKK3-induced AP1 and CHOP Activation and Induces Apoptosis *. *J. Biol. Chem.* **2004**, *279*, 17278–17282, doi:10.1074/jbc.C400063200.
 15. Ye, H.; Arron, J.R.; Lamothe, B.; Cirilli, M.; Kobayashi, T.; Shevde, N.K.; Segal, D. Distinct molecular mechanism for initiating TRAF6 signalling. *Nat. Publishing Gr.* **2002**, *418*, 443–447.
 16. Poblenz, A.T.; Jacoby, J.J.; Singh, S.; Darnay, B.G. Inhibition of RANKL-mediated osteoclast differentiation by selective TRAF6 decoy peptides. *Biochem. Biophys. Res. Commun.* **2007**, *359*, 510–515, doi:10.1016/j.bbrc.2007.05.151.
 17. Thévenet, P.; Shen, Y.; Maupetit, J.; Guyon, F.; Derreumaux, P.; Tufféry, P. PEP-FOLD : an updated de novo structure prediction server for both linear and disulfide bonded cyclic peptides. **2012**, *40*, 288–293, doi:10.1093/nar/gks419.
 18. Shen, Y.; Maupetit, J.; Derreumaux, P. Improved PEP-FOLD Approach for Peptide and Miniprotein Structure Prediction. *JCTC - J. Chem. Theory Comput.* **2014**.
 19. Lamiable, A.; Thévenet, P.; Rey, J.; Vavrusa, M.; Derreumaux, P.; Tuff, P. PEP-FOLD3 : faster denovo structure prediction for linear peptides in solution and in complex. **2016**, 1–6, doi:10.1093/nar/gkw329.
 20. Singh, S.; Singh, H.; Tuknait, A.; Chaudhary, K.; Singh, B.; Kumaran, S.; Raghava, G.P.S. PEPstrMOD : structure prediction of peptides containing natural , non-natural and modified residues. *Biol. Direct* **2015**, 1–19, doi:10.1186/s13062-015-0103-4.
 21. Kaur, H.; Garg, A.; Raghava, G.P.S. PEPstr: A de novo Method for Tertiary Structure Prediction of Small Bio- active Peptides. *Bentham Sci. Publ.* **2007**, 626–631.
 22. Zhang, Y. I-TASSER server for protein 3D structure prediction. *BMC Bioinformatics, BioMed Cent.* **2008**, *8*, 1–8, doi:10.1186/1471-2105-9-40.
 23. Roy, A.; Kucukural, A.; Zhang, Y. I-TASSER: a unified platform for automated protein structure and function prediction. *Nat. Publ. Gr.*

- 2010**, **5**, 725–738, doi:10.1038/nprot.2010.5.
24. Yang, J.; Yan, R.; Roy, A.; Xu, D.; Poisson, J.; Zhang, Y. The I-TASSER Suite : protein structure and function prediction. *Nat. Publ. Gr.* **2015**, **12**, 7–8, doi:10.1038/nmeth.3213.
 25. Sippl, M.J. Recognition of Errors in Three-Dimensional Structures of Proteins. *Wiley Online Libr.* **1993**, **362**, 355–362.
 26. Wiederstein, M.; Sippl, M.J. ProSA-web : interactive web service for the recognition of errors in three-dimensional structures of proteins. *Natl. Libr. Med. Natl. Cent. biotechnology Information, PubMed* **2007**, **35**, 407–410, doi:10.1093/nar/gkm290.
 27. Van Zundert, G.C.P.; Rodrigues, J.P.G.L.M.; Trellet, M.; Schmitz, C.; Kastiris, P.L.; Karaca, E.; Melquiond, A.S.J.; Van Dijk, M.; De Vries, S.J.; Bonvin, A.M.J.J. The HADDOCK2.2 Web Server: User-Friendly Integrative Modeling of Biomolecular Complexes. *J. Mol. Biol.* **2016**, **428**, 720–725, doi:10.1016/j.jmb.2015.09.014.
 28. Honorato, R. V.; Koukos, P.I.; Jiménez-García, B.; Tsaregorodtsev, A.; Verlato, M.; Giachetti, A.; Rosato, A.; Bonvin, A.M.J.J. Structural Biology in the Clouds: The WeNMR-EOSC Ecosystem. *Front. Mol. Biosci.* **2021**, **8**, 1–7, doi:10.3389/fmolb.2021.729513.
 29. Bjellqvist, B.; Hughes, G.J.; Hochstrasser, D. The focusing positions of polypeptides in immobilized. *Electrophoresis* **1993**, **14**, 1023–1031.
 30. Bjellqvist, B.; Basse, B.; Olsen, E.; Celis, J.E. Reference points for comparisons of two-dimensional maps of proteins from different human cell types defined in a pH scale where isoelectric points correlate with polypeptide compositions. *Electrophoresis* **1994**, **15**, 529–539, doi:10.1002/elps.1150150171.
 31. Ning, J.; Yu, Z.; Xie, H.; Zhang, H.; Zhuang, G.; Bai, Z.; Yang, S.; Jiang, Y. *ExPASy: The proteomics server for in-depth protein knowledge and analysis.*; 2008; Vol. 24; ISBN 1588293432.